

RBE with Non-Poisson Distribution of Radiation Induced Strand Breaks

M. Loan^{a,b*}, M. Alameen^c, A. Bhat^d and M. Tantary^e

^a*Department of Physics, Kuwait College of Science and Technology, 28007, Kuwait*

^b*ANUC, Australian National University, Canberra, 2000, Australia*

^c*Department of Mathematics, Australian College of Kuwait, 13015, Kuwait*

^d*Department of Radiation Oncology, Clinch Valley Medical Center, Richlands, Virginia, 24641, USA*

^e*Department of Internal Medicine, Clinch Valley Medical Center, Richlands, Virginia, 24641, USA*

(Dated: September 16, 2020)

Postulating that increasing linear energy transfer (LET) causes non-random clustering of lethal lesions to deviate from the Poisson distribution, we employ a non-Poisson approach as a more flexible alternative that accounts for overdispersion of lethal lesions. Using non-homologous end-joining (NHEJ) pathway of double-strand break repair, a customized negative binomial (NB) distribution is used to describe the distribution of lethal events in a cell nucleus. The proposed model provides a novel, mechanistically based explanation for the measured values of the biological relevant quantities, such as model parameters and relative biological effectiveness (RBE) of the surviving cells, for various light ion types and LET values. The estimated quantities are compared with the predictions of several mechanism-inspired models and experimental data at medium and high LET values. The results examined are closer to the Microdosimetric-Kinetic model predictions for helium and carbon ions but progressively lower than trends predicted by the Local Effect Model and the Repair-Misrepair-Fixation model in the large LET region. The results support the view that the limitation in the increase in RBE at high LET can be accounted for entirely, or, in large part, by clustering of lethal events to cause deviation from the Poisson distribution.

Keywords: linear quadratic model, DNA damage, RBE, hadrontherapy

I. INTRODUCTION

It has long been established that the linear-quadratic (LQ) model is a good approximation to a wide range of damage-kinetic models which describe the kinetics of DNA double-strand breaks (DSBs) and other basic lesions [1–7]. Underlying the application of these kinetic-models to fractionation effects is pairwise misrepair of primary lesions such as DSBs or base damage. The double-strand breaks are resolved either through restitution or binary misrepair. At typical radiotherapeutic doses, most DSBs are removed by restitution, which results in the classic linear-quadratic dose dependence. At very high doses per fraction, binary misrepair can dominate, which results in a linear relation between effect and dose. Overall, these mechanisms produce a linear-quadratic-linear dose-response relationship, as has been pointed out by many authors [8–11]. Detailed experimental studies in vivo cell survival suggested that all these data are consistent with the Linear-Quadratic (LQ) model up to about 20 - 24 Gy [12–16]. In vitro cell survival, the quality of fit to the LQ model does not decline significantly until doses above 15 Gy are included [17]. Theoretical estimates, on the other hand, gauged the practical applicability of LQ approximation at dose below 17 Gy and suggested corrections to the LQ model at higher doses [3]. Various other mechanistic models describing pairwise production of chromosome aberrations predict virtually the same time-dose relations as does the LQ approach [18–22].

Although different models have different formulations for the dose dependence of the mean lethal lesion yield, the common feature of the approaches used in these models is that error distribution around the mean number of lethal lesions per cell is assumed to be Poisson. Such assumptions are understandable, given that these models evolved to explain clonogenic cell survival, an endpoint for which the number of lesions in individual cells cannot be quantified. Additionally, the linear relationship of RBE and LET is consistent with the experimental values for LETs low enough that the radiation induced lethal lesions are Poisson distributed among the cells of the irradiated population [20, 23]. This linearity allows extrapolation to values of LET greater than the range for which there is Poisson distribution of lethal lesions. However, despite widespread usage of the LQ, there remain questions about departure of its linear quadratic relation from the experimental survival values [24]. The experimentally measured RBE with increasing LET becomes progressively less than that of the linear increase established for $\text{LET} < 70 \text{ keV}/\mu\text{m}$ [25]. This could be due to the deviation of the distribution of lethal lesions among the irradiated cells from that of the Poisson distribution. Whereas for sparsely-ionizing radiation below $\sim 50 \text{ Gy}$ per fraction, the deviations from a Poisson distribution are quite minor [3, 26], the deviations of lethal lesions from Poisson distribution are significant at high LETs [24, 27–29].

* Corresponding author

This is evident from chemical and biological factors, such as heterogeneity of DSB complexities, the existence of multiple DSB repair pathways with different fidelities as well as from the microdosimetric considerations for ionizing radiations such as hadrons and heavy ions at higher LETs and doses [25, 30–32]. It is plausible to hypothesize that these processes can lead to overdispersion which can change the predicted cell survival curve shape.

As a result, many investigators have raised questions about the general validity of the LQ, and whether it truly represents underlying biology or is simply a useful empirical tool [28, 29, 33]. The discrepancy between experimental survival and the linear quadratic model at higher dose is explained by heterogeneity of sensitivity to radiation among the cells of the irradiated population [33]. Reported increase in local multiplicity of radiation-induced strand-breaks with increasing LET could constitute such a change in lesion structure [34, 35] as well as a decrease in DSB yield for $\text{LET} > 100 \text{ keV}/\mu\text{m}$ [36]. In addition to the shift in maximum of RBE, the resulting RBE is estimated to be less than indicated by extrapolation of the linear relationship to higher LET values [27, 29]. Postulating that increasing LET causes non-random clustering of lethal lesions in some cells to deviate from the Poisson distribution, we use a non-Poisson distribution as a more flexible alternative that allows to accommodate a variety of mechanisms for overdispersion. Other non-Poisson distributions used to target overdispersion that affects the predicted dose response for cell survival include, for example, the Neyman distribution, which accounts for stochasticity of the number of ionizing track traversals per cell and the number of chromosomal aberrations per track [37–39]. We employ a customized negative binomial (NB) distribution to derive an equation that predicts the model parameters which are used to estimate RBE of V79 cell lines radiated by charged hadrons with different physical parameters. The dependence of the predicted RBE on LET is compared with the results obtained from the Local Effect Model (LEM) [40, 41], the Microdosimetric-Kinetic (MK) Model [42, 43], and the Repair-Misrepair-Fixation (RMF) Model [44–46]. The estimated RBE behaviour, in principle, may offer a clinically useful approach for modelling the effects of high doses per fraction at large LET.

II. NON-POISSON DISTRIBUTION OF LETHAL LESIONS

A. Model and Method

Assuming the lethal lesions are Poisson distributed from cell to cell, the surviving probability of a cell is given by

$$S = e^{-Y} = e^{-\alpha D - G\beta D^2}, \quad (1)$$

where Y is the yield of lethal lesions, α and β are parameters describing the cell's radiosensitivity, and G is the generalized Lea-Catcheside time factor, which accounts quantitatively for fractionation/protraction. It has been well established that the effective plot of Eq. (1), on a log scale, gives what is referred to as a "shouldered" dose response curve. The initial region of the curve is dominated by the linear term at low doses, followed by increasing curvature as the quadratic term becomes more significant. The degree of curvature is commonly expressed in terms of the α/β ratio or cellular repair capacity (CRC) and corresponds to the dose at which the linear and quadratic contributions are equal. Thus, cells with high CRC see a relatively constant rate of cell killing with increasing dose, while those with a low CRC show a pronounced curvature. Assuming that there is no reduction in cell killing due to repair ($G = 1$), the simplest single-fraction LQ formalism takes the form:

$$S = e^{-\alpha D - \beta D^2}.$$

Also, assuming that the distribution of lethal chromosomal lesions among individual human cells exposed to light ion irradiation is somewhat overdispersed, we employ a customized negative binomial (NB) distribution for evaluating the probability of observing k lethal lesions in a cell

$$P_{NB}(k) = \frac{\Gamma(k + 1/r)}{\Gamma(1/r) \times k!} \left(\frac{1}{1 + r\mu} \right)^{1/r} \times \left(\frac{1}{1 + 1/r\mu} \right)^k. \quad (2)$$

Specifying the distribution in terms of its mean, $\mu = \lambda = (1 - p)r/p$, the variance is described by the convenient expression $\mu + \mu^2/r = \mu + \omega\mu^2$, where either the parameter r or its reciprocal ω is referred to as the over-dispersion parameter. Consequently, if $\omega \rightarrow 0$, there is no over-dispersion and the variance and mean are equal, as in the Poisson distribution. On the other hand, if $\omega > 0$, the variance becomes greater than the mean and the ratio of variance to mean increases as the mean increases. The same approach is extended to model the mean yield Y of lethal lesions per cell after a radiation dose D , with the cell surviving fraction S defined as the probability of zero lethal lesions as:

$$S_{IP} = P_{NB}(0) = (1 + rY)^{-1/r}. \quad (3)$$

Following [47], the radiation-induced DSBs in the nucleus and probability of cell death can be predicted by first calculating the average number of primary particles that cause DSB, n_p , and the average number of DSBs yielded by each primary particle that causes DSB, λ_p . The DSB yield per cell per primary particle is given by $\lambda = N/n$, where $N = YD$ is the average number of radiation-induced DSBs per cell and n is the number of the particles passing through the cell nucleus. Assuming that the number of DSBs yielded by a primary particle is distributed according to NB distribution, Eq. (2), the probability of a primary particle passing through a nucleus without causing any DSB is given by

$$P_{NB}(k=0) = (1 + r\lambda)^{-1/r}. \quad (4)$$

The average number of primary particles that cause DSB, and the average number of DSBs yield per primary particle that causes DSB are respectively given by

$$n_p = n[1 - (1 + r\lambda)^{-1/r}], \quad (5)$$

$$\lambda_p = \frac{\lambda}{[1 - (1 + r\lambda)^{-1/r}]}. \quad (6)$$

The repair of the breaks is modelled by the non-homologous end-joining (NHEJ) pathway [48] with the overall behaviour given by

$$N_{avg} = \mu_y N \times (1 - P_{correct}), \quad (7)$$

where N_{avg} is the average number of lethal events, μ_y is the sensitivity of an error repair, and $P_{correct}$ is the total probability of a DSB being correctly repaired. For any break in a particular condition, the true distribution of rejoining rates is a non-trivial and complex function and lacks a simple distribution for its overall distribution. Following [47, 49], the repair behaviour is approximating the recombination function as a step function

$$f(x) = \begin{cases} 1 & \text{if } x \leq d_{max} \\ 0 & \text{elsewhere,} \end{cases}$$

where d_{max} is some maximum separation between the break ends. This simplifies the probability of correct repair for a given break to $1/(1+k)$, where k is the number of breaks within the distance d_{max} [49]. Assuming that the breaks within the spherical radius are NB distributed, the expectation value that a randomly chosen break will repair correctly (a DSB end do not be joined with a DSB end from a DSB induced by a different primary particle) is given by (see the appendix)

$$P_1 = \frac{1}{\mu_{int}(1-r)} \left[1 - (1 + r\mu_{int})^{1-1/r} \right], \quad (8)$$

where $\mu_{int} = \eta(\lambda_p)n_p$ is the average probability of a DSB end being joined with a DSB end from a DSB induced by a different primary particle and η is the effective integral misrejoining probability for a single randomly chosen DSB within a radius.

Also, assuming that a primary particle generates DSBs randomly on it's track, the probability that a DSB end not be joined with a DSB end from a different DSB induced by the same primary particle is given by

$$P_2 = \frac{1}{\mu_{track}(1-r)} \left[1 - (1 + r\mu_{track})^{1-1/r} \right], \quad (9)$$

where $\mu_{track} = \phi\lambda_p$ is the average probability of a DSB end being joined with a DSB end from a DSB induced by the same primary particle. Therefore, the total probability of a DSB being correctly repaired is given by

$$\begin{aligned} P_{correct} &= \mu_x P_1 P_2 \\ &= \mu_x \left[\frac{\omega}{\mu_{int}(\omega-1)} \left(1 - (1 + r\mu_{int})^{1-\omega} \right) \right] \times \left[\frac{\omega}{\mu_{track}(\omega-1)} \left(1 - (1 + r\mu_{track})^{1-\omega} \right) \right], \end{aligned} \quad (10)$$

where μ_x is process-specific fidelity. The first term in the square brackets quantitatively describes the interaction of DSBs induced by different primary particles and the second term in square brackets describes the effect of clustered DNA damage.

Using the above repair probabilities, Eq. (7) becomes

$$N_{avg} = \mu_y N \times \left[1 - \mu_x \left\{ \frac{\omega}{\mu_{int}(\omega - 1)} \left(1 - (1 + r\mu_{int})^{1-\omega} \right) \right\} \right. \\ \left. \times \left\{ \frac{\omega}{\mu_{track}(\omega - 1)} \left(1 - (1 + r\mu_{track})^{1-\omega} \right) \right\} \right], \quad (11)$$

where μ_y is the sensitivity of error repair. The cell survival becomes

$$S_{NB} = \left(1 + rN_{avg} \right)^{-1/r} = \left(1 + r(\alpha D + \beta D^2) \right)^{-1/r}, \quad (12)$$

where

$$\alpha = \mu_y Y \left[1 - \mu_x \frac{\omega}{\phi \lambda_p (\omega - 1)} \left(1 - (1 + r\phi \lambda_p)^{1-\omega} \right) \right] \\ \beta = \frac{1}{2} \frac{\eta(\lambda_p)}{\lambda_p} \mu_x \mu_y Y^2 \frac{\omega}{\phi \lambda_p (\omega - 1)} \left(1 - (1 + r\phi \lambda_p)^{1-\omega} \right) \quad (13)$$

are the improved parameters of the model. The values of μ_x, μ_y, ξ, ϕ and $\eta_{\lambda_p \rightarrow 1}$ obtained with the experimental data of linear parameter values and $\eta_{\lambda_p \rightarrow \infty}$ with the experimental data of β values of the survival curves are adapted from Wang et al [47].

The yield of DSBs induced by ionizing radiations was calculated with fast Monte Carlo damage simulation (MCDS) software [50]. This algorithm captures the trend in DNA damage spectrum with the possibility that the small-scale spatial distribution of elementary damages is governed by stochastic events and processes [51, 52]. The use of this quasi-phenomenological algorithm is to provides nucleotide-level maps of the clustered DNA lesions and to avoid the initial simulation of the chemical processes. It has been observed that MCDS algorithm gives reliable results of the damage yields that are comparable to those obtained from computationally expensive but more detailed track structure simulations. For MCDS simulations, the results of DNA damage yields for protons and light ions are usually obtained within minutes. We generate ten ensembles of DSB yield measurements for each LET value for later analysis. The expectation values and statistical error estimates of the observables were estimated using the jackknife method. The statistical errors were estimated by grouping the stored measurements into 5 bins, and then the mean and standard deviation of the final quantities were estimated by averaging over the bin averages. The estimate of the error of observable ρ was calculating by using

$$\delta\rho = \sqrt{\frac{M-1}{M} \sum_{m=1}^M (\bar{\rho}_m - \langle \rho \rangle)^2}.$$

Statistical significance between two data sets was accessed using a 2-tail t -test with a 95% confidence interval.

B. Particle RBE Characterization

Whereas a large amount of data from different experimental protocols and biological models are available [53], the adoption of a simple and unique RBE-LET relationship in effective treatment planning is surrounded by a number of uncertainties. Few studies have supported a reasonable approximation of fixed RBE to describe the increased effectiveness of light ions [54–57], the concerns for a better understanding of RBE-LET relationship for significant clinical relationship have been raised. The modelled parameters α and β for the same type of cells irradiated by different radiation types at different LET can be used to reflect on the relative biological effectiveness (RBE). The RBE for cell killing by high LET radiation is conventionally defined in terms of the ratio of the low LET reference radiation, $(\alpha/\beta)_x$, to the high LET dose producing the same survival fraction. However, it is convenient to focus on the RBE in terms of its asymptotic values. Following [58], we consider the effect of changed production of sub-lethal damage with varying LET by incorporate the twin concepts of RBE_{max} and RBE_{min} , which represent the asymptotic values of RBE in the limit of 0 and ∞ dose, respectively. In these limits,

$$RBE_{max} = \alpha/\alpha_x, \quad RBE_{min} = \sqrt{\beta/\beta_x},$$

where α and β are given by Eq.(13). The resulting expression for RBE is given by [58]

$$RBE = (-(\alpha/\beta)_x + \sqrt{\Gamma})/2D_{ion}, \quad (14)$$

where

$$\Gamma = (\alpha/\beta)_x^2 RBE_{max}^2 + 4(\alpha/\beta)_x RBE_{max} D_{ion} + 4RBE_{min}^2 D_{ion}^2.$$

We expect the over-dispersion of lethal lesions to affect the predicted RBE at high LET and doses.

III. RESULTS AND DISCUSSION

A. Trends in Radiosensitivity with Particle LET

Figures 1 and 2 show the estimated radiosensitivity parameters using protons, helium and carbon ions over a wide range of LET values with the reference radiosensitivity parameters $\alpha_x = 0.38 \text{ Gy}^{-1}$ and $\beta_x = 0.038 \text{ Gy}^{-2}$. The general trends in the linear parameter are similar between the proton and helium-ions, with the measured parameters reaching their respective maximum between $80 \text{ keV}/\mu\text{m}$ and $200 \text{ keV}/\mu\text{m}$. At higher LET, the α parameter for helium ions is higher than that for the protons and carbon ions. The linear parameter for carbon ions seems to increase to a maximum before starting to fall, with the fall-off shifting to higher LET. In terms of the absolute values, we observe significant variations in our linear estimates at low LET values. This may be due to the non-Poisson distribution based description of the model parameters within our framework.

A comparison of the predicted linear parameter results for helium and carbon ions with measured data published by Furusawa et al. [59] (Fig. 2) shows an underestimation for helium ions for $\text{LET} > 50 \text{ keV}/\mu\text{m}$ but a reasonable agreement for carbon ions in both low and high LET regions. Comparison with the LEM IV, RMF, and MK models [60] shows that our estimates for protons deviate significantly from the predictions of these models, which predict substantially large α values with a general trend towards a monotonic increase in α values with increasing LET. For helium ions, our results are comparable, within errors, with the RMF model and show a comparable trend with MK model for $\text{LET} > 60 \text{ keV}/\mu\text{m}$. Our α values for carbon ions seem to agree with those predicted by MK model for $\text{LET} > 200 \text{ keV}/\mu\text{m}$. The near agreement with MK model predictions is not surprising since the distribution of initial DSB in MK model is effectively formulated as a non-Poisson distribution. The downward trends in α within the framework of LEM IV model is thought to be due to the proximity effect for DSB clustering [61].

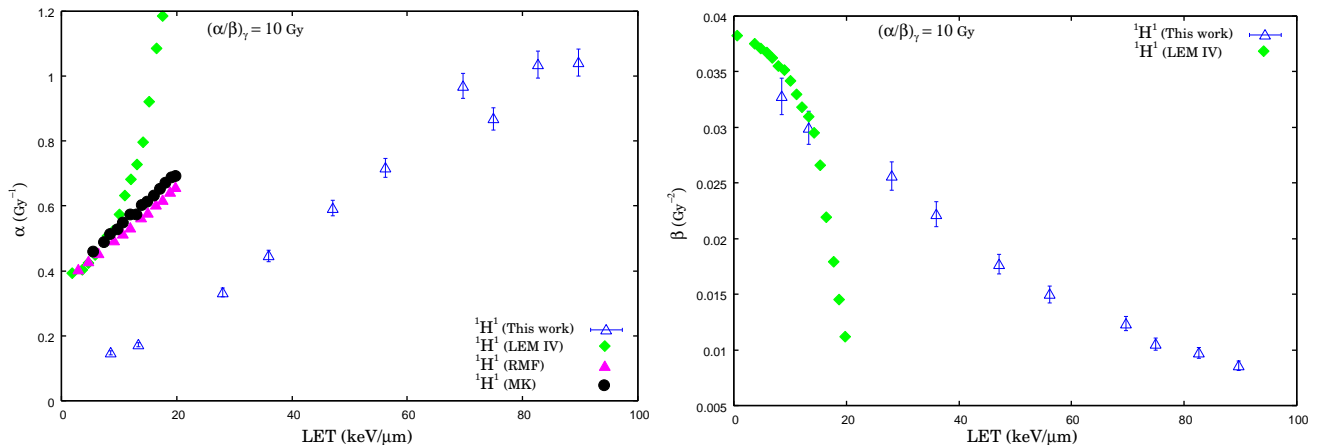


FIG. 1: Distribution of linear-quadratic parameters of the model exposed to helium and carbon ions for a range of LET values. For comparison, the predictions of the LEM IV, RMF, and MK models [60] are also shown.

The quadratic parameter values suggest a decreasing trend with increasing LET for all ion species explored here. The predicted trend is in contrast with the LEM IV model which predicts a sharp drop in β value that eventually approaches zero with increasing LET. Such a trend is attributed to the simultaneous decrease in the track diameter with decreasing energy and the increase in the inter-track distance among DSB with increasing LET [60]. The MK and RMF model predictions are not included for comparison since in MK model β is considered to be LET independent and RMF predicts a continuous increase in β with LET which is in contrast with the model analysis of the data from

the Particle Irradiation Data Ensemble (PIDE) database that suggests a decreasing trend of β with increasing LET. However, the quantitative analysis of such trends is needed to draw a definite conclusion.

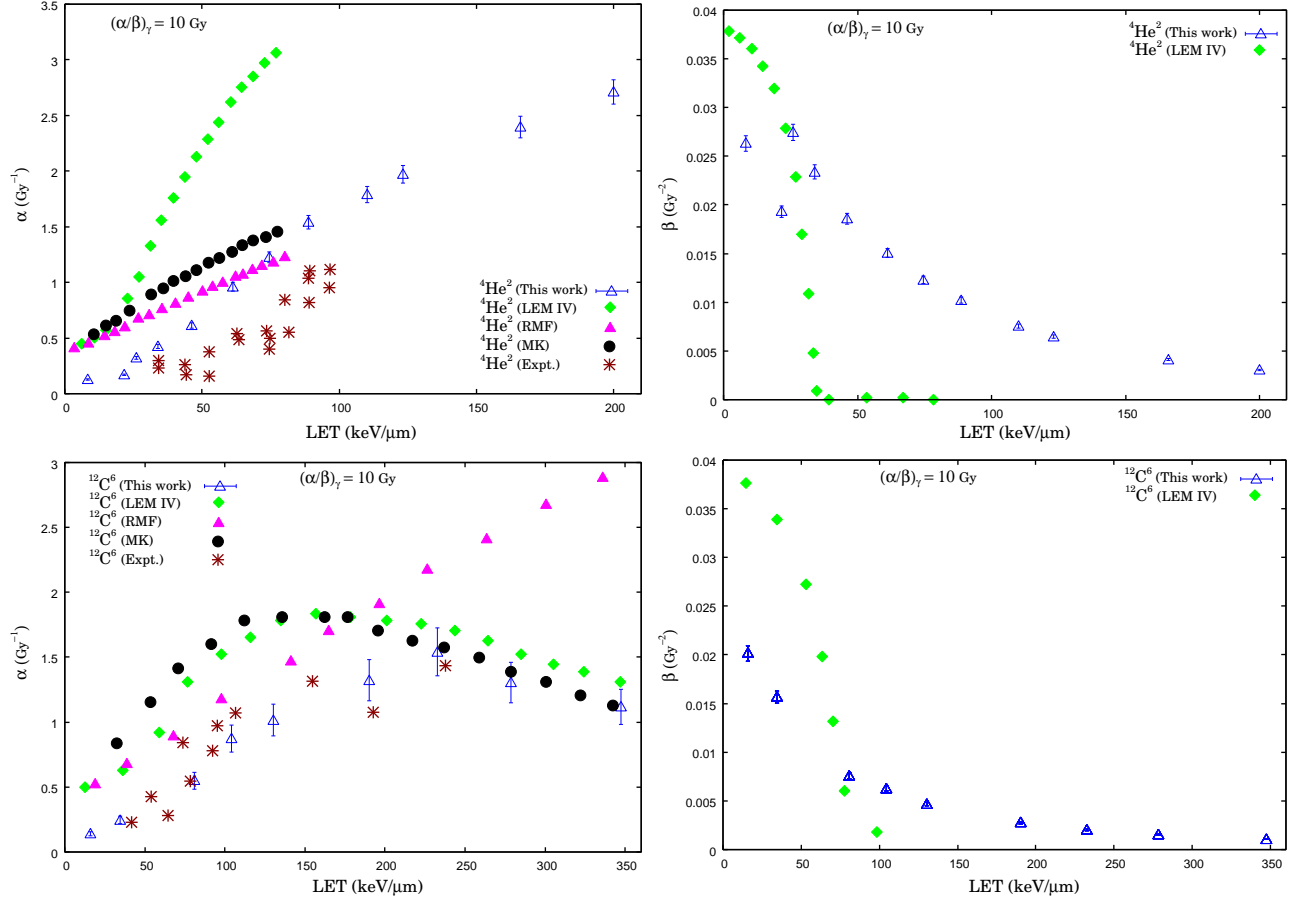


FIG. 2: Distribution of linear-quadratic parameters of the model exposed to protons and helium ions for a range of LET values. The experimental results of the linear parameter using He-3 and carbon ions for a V79 cell [59] are shown with solid circles. For comparison, the predictions of the LEM IV, RMF, and MK models [60] are also shown.

It is obvious from the effective plots that LET strongly affects linear coefficient than quadratic parameter. It is now generally accepted that high-LET radiation induces complex clustered damage to DNA, particularly complex DSBs [62–65], which are less repairable by either non-homologous end-joining or the homologous recombination pathway [66]. If complex DSBs are more persistent and more likely to be misrepaired, one might expect the beta term to increase as the LET increases.

To explore the effect of the cell sensitivity on cell killing for charged particle species, we study the ratio α/β which is mainly attributed to the number of primary particles that cause DSBs per dose for charged particles at given LET values. Fig. 3 shows the ratio α/β for V79 cells irradiated by helium and carbon ions at different LET along with the experimental data from [59]. We observe that the slope of the ratio increase steeply with increasing LET. As mentioned above, this could be due to increase in α due to the clustered DNA damage effect as well as the decrease in the interaction of DSBs induced by different primary particles. This interaction becomes vanishingly small at intermediate LET values. We also notice that the ratio tends to reach more or less a plateau (not shown in the figure) for carbon ions at $\text{LET} > 280 \text{ keV}/\mu\text{m}$. This might be due to the saturation in the clustered DNA damage and the effect of overkill on cell death.

B. RBE Results

To further explore the impact of LET on radio-sensitivity, we analyse the RBE corresponding to the initial slope for different particle types. Figure 4 collects and compares the predicted RBE-LET spectra, at $(\alpha/\beta)_R = 10 \text{ Gy}$, with the theoretical and experimental results for different radiation species. The proton RBE shows approximately a linear

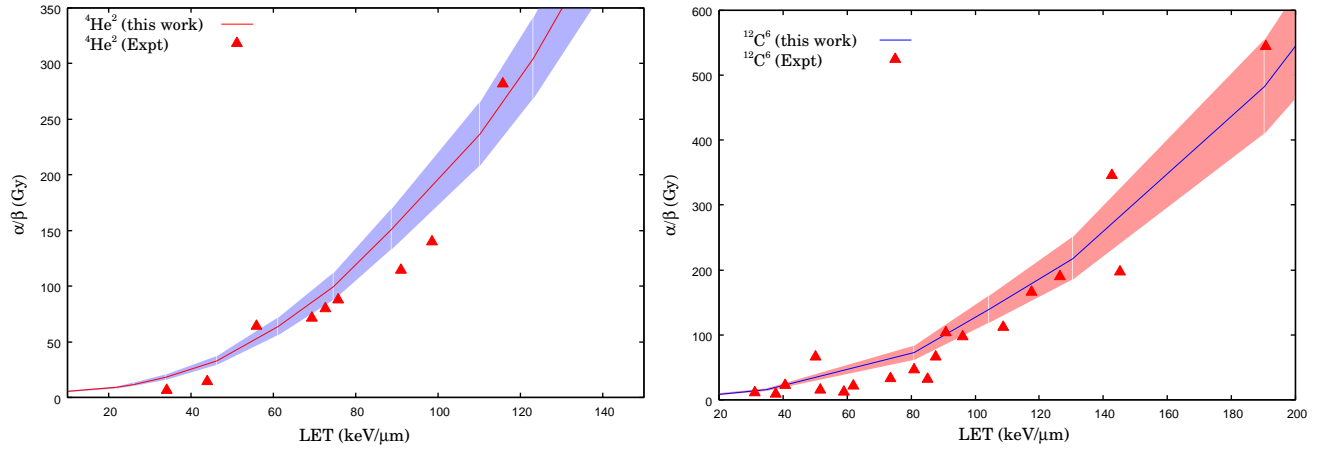


FIG. 3: Comparison of modelled results (solid line) and experimental data (solid triangles) [59] of α/β ratio for V79 cells for helium and carbon ions.

LET dependance for $\text{LET} < 60 \text{ keV}/\mu\text{m}$ with a peak value of approximately 1.71 ± 0.06 at around $80 \text{ keV}/\mu\text{m}$. A comparison between our estimates and the observed values shows that in addition that the magnitude of the RBE peak value is relatively small than the experimental value (1.86), the peak appears to occur at much higher LET compared to the experimental peak at $50 \text{ keV}/\mu\text{m}$ [59]. However, this is as expected since the experimentally measured RBE follows a linear relation with LET for LET less than a value that lies in the range of $40 - 90 \text{ keV}/\mu\text{m}$ [23].

Another comparison of our results with the studies performed by Stewart et al [60] indicates different levels of disagreement in RBE in low LET region at threshold dose value of 10 Gy for protons. The most likely reason for the disagreement is the spatial distribution mechanism of initial DSBs (approximated by a Poisson distribution) which has a significant impact on the RBE for cell survival [52]. Whereas for low-LET ($< 50 \text{ keV}/\mu\text{m}$), the average number of potentially lethal DSB per track is small, the induction of DSB can be safely approximated by the Poisson distribution, increasing LET causes deviation from the Poisson distribution by non-random clustering of lethal lesions in some cells. This deprives other cells of a lethal lesion and allows them to survive. This causes the measured values of RBE to be lower than those indicated by the LEM-IV and MRF models for higher LET. This structural change may also induce an alteration in the rate of repair of lesions that undergo transformations, thus increasing the yield of strand breaks. Reported increase in local multiplicity of radiation-induced strand-breaks with increasing LET could constitute such a change in lesion structure [34, 35] as well as a decrease in DSB yield for $\text{LET} > 100 \text{ keV}/\mu\text{m}$ [36]. In addition to the shift in maximum of RBE, the resulting RBE is estimated to be less than indicated by extrapolation of the linear relationship to higher LET values [27, 29].

For helium and carbon-ions, the predicted RBE shows a non-linear behaviour for LET range explored here. The difference in the RBE is significant in medium and high LET regions. An LET almost twice as high is required to obtain the same RBE for helium and carbon ions. Whereas the initial yield of DSBs is slightly higher from helium ions than from carbon ions at the same LET in low LET region, the biological effectiveness seems to be greater for helium ions than in carbon ions. Similar results have been reported using low-energy light ions [67]. This can be attributed to the difference in the track structures of the ions at the same LET through the differences in the velocity and effective charges of the ion. Comparison with the mechanistic models [60] shows that the predicted values for helium RBE cell survival are closer to the MK model values in the medium and large LET region. This is as expected since the MK model incorporates the effect of deviation from the Poisson distribution to a compound Poisson distribution at higher LET. For carbon ions, the deviation of the predicted values from those of the mechanistic models is significant in low LET region. Again, this is as expected since for low-LET radiations since a non-Poisson distribution for the induction of DSB is reduced to a Poisson distribution of primary tracks passing through the cell that determines the distribution of initial damage [52]. The predicted values, however, are comparable, within errors, with RMF and MK models in the high-LET region. The predicted RBE values show no significant dose dependence for the absorbed dose $< 3 \text{ Gy}$, at low LET values for helium ions (Fig. 4 bottom right panel). Whether this trend continues for reference radiation with lower $(\alpha/\beta)_R$ remains to be explored.

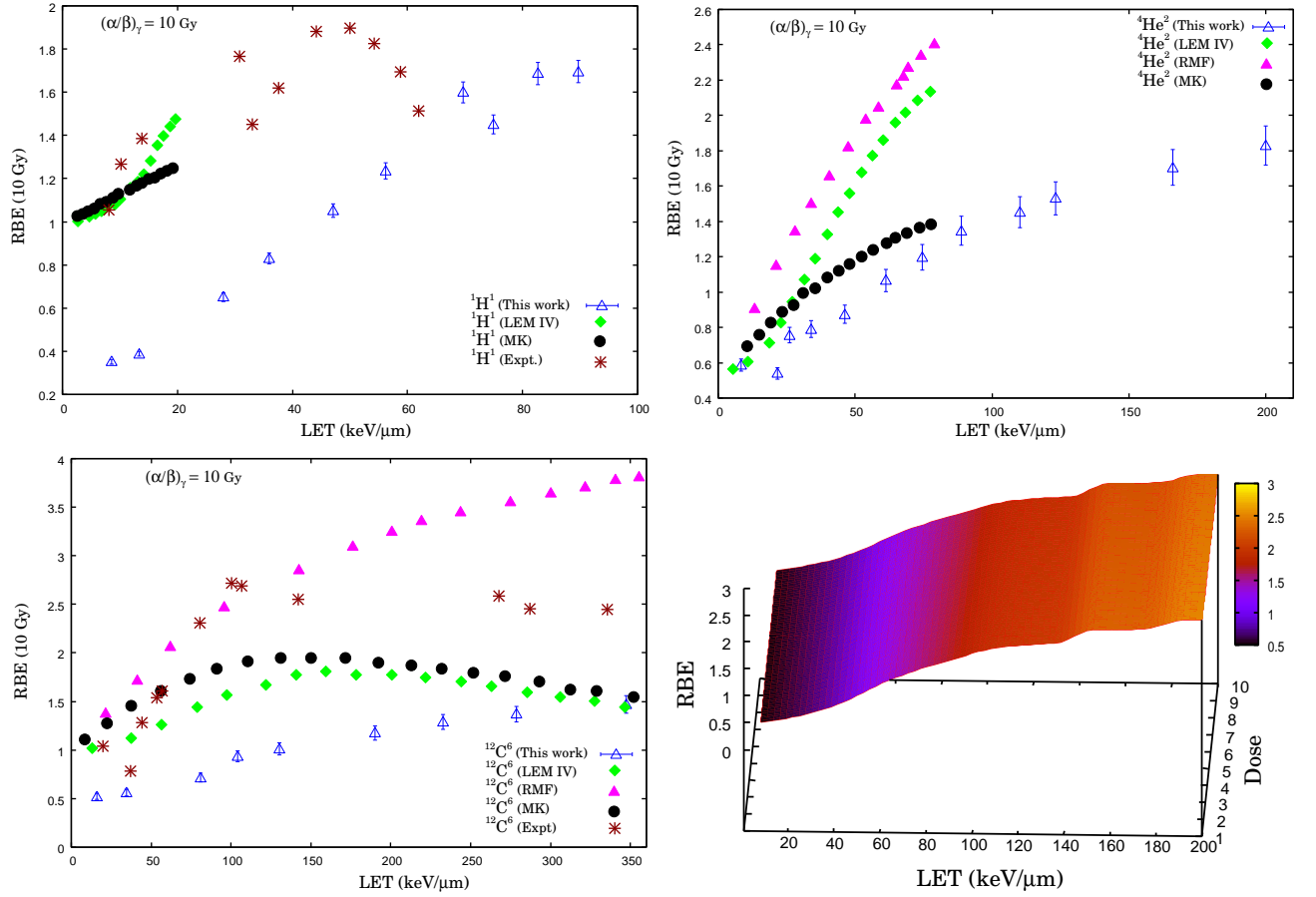


FIG. 4: Comparison between estimated values of RBE and modelled values of the the LEM IV, RMF, and MK models [60] at 10 Gy dose. Also, are shown the observed RBE values from cell survival experiments at 10% survival for V79 cells [59].

IV. CONCLUSIONS

Whereas, for low LET values with an average of less than one lethal lesion per primary particle traversal, the experimental values of RBE coincide with the RBE-LET linear relationship, the measured RBE values are progressively lower than the predictions of the RBE-LET linear extrapolation at higher LET values. This decrease in the measured RBE values for high-LET radiations is an indicator to associate the distribution of lethal lesions to non-Poisson distributions that correlate closely with biological effects. To account for the damage saturation correction, we adopted the effect of a customized negative binomial distribution of lethal lesions as a more flexible approach that accounts for the non-random clustering and overdispersion of lethal lesions to evaluate the variation of RBE of proton, helium and carbon ions at higher LET. We postulated that increasing LET causes deviation from the Poisson distribution of lethal lesions in some cells, thereby causing a decrease in the measured values of RBE for higher LET. We developed an equation that estimated the linear and quadratic parameters of the model as well as the deviation of RBE that is expected to occur because of the negative binomial distribution of lethal lesions. The suggested deviation was supported by observed increase α and β with increasing LET for LET below the maximum as well as by decreasing α and β for LET above the maximum.

In conclusion, the decrease in estimated RBE at high LET can be attributed to clustering on lethal lesions in some cells causing deviation from the Poisson distribution. The RBE results indicate that the more sensitive cells are to radiation at low LET, lower will be peak on RBE they attain as LET increases. Nonetheless, the non-Poisson distribution implemented seemed to be consistent with previously reported data for the variation of initial slope of survival curves and RBE at high LET values of different radiation species. However, it is not possible to draw a definite conclusion since the tissue dependence of RBE, which is reflected in parameter value of reference radiation, was not explored in this study. While assigning a high $(\alpha/\beta)_x$ value to the target that actually might have a low reference parameter value will underestimate RBE, since for low $(\alpha/\beta)_x$ the average RBE could be higher. For a conclusive

signature of non-Poisson distribution of lethal lesions, work is under way to investigate the impact of a more accurate distribution that could result in an improved model with realistic properties overall.

Acknowledgments

We are grateful for access to computing facility at the Kuwait College of Science and Technology. ML is thankful to A. Yousef at the Department of Mathematics, KCST, for a number of valuable suggestions which provided the impetus for much of this work.

-
- [1] M. Guerrero, R. Stewart, J. Wang and X. Li, *Equivalence of the linear-quadratic and two-lesion kinetic models*, Phys. Med. Biol. **47**, 3197 (2002)
 - [2] R. Preston, *Mechanisms of induction of specific chromosomal alterations*, Basic Life Sci. **53**, 329 (1990)
 - [3] R. Sachs, P. Hahnfeldt, and D. Brenner, *The link between low-LET dose-response relations and the underlying kinetics of damage production/repair/misrepair*, Int. J. Radiat. Biol. **72**, 351 (1997)
 - [4] L. Gerweck, S. Zaidi, A. Zietman, *Multivariate determinants of radiocurability. I: Prediction of single fraction tumor control doses*, Int. J. Radiat. Oncol. Biol. Phys. **29**, 57 (1994)
 - [5] H. Thames, *An incomplete-repair model for survival after fractionated and continuous irradiations*, Int. J. Radiat. Biol. **47**, 319 (1985)
 - [6] M. Brown, *et al.*, *Comment on Tumor response to radiotherapy regulated by endothelial cell apoptosis (II)*, Science, **302**, 1894 (2003)
 - [7] R. Stewart, *Two-Lesion Kinetic Model of Double-Strand Break Rejoining and Cell Killing*, Radiat. Res. **56**, 365 (2001)
 - [8] H. Rossi and M. Zaider, *in Quantitative Mathematical Models in Radiation Biology*, edited by J. Kiefer Springer, New York, 1988, pp. 111 - 118.
 - [9] D. Brenner, *Track structure, lesion development, and cell survival*, Radiat. Res. **124**, S29 (1990)
 - [10] T. Radivoyevitch, D. Hoel, A. Chen, and R. Sachs, *Misrejoining of double-strand breaks after X irradiation: Relating moderate to very high doses by a Markov model*, Radiat. Res. **149**, 59 (1998)
 - [11] M. Carlone, D. Wilkins, and P. Raaphorst, *The modified linear-quadratic model of Guerrero and Li can be derived from a mechanistic basis and exhibits linear-quadratic-linear behaviour*, Phys. Med. Biol. **50**, L9 (2005)
 - [12] G. Barendsen, *Dose fractionation, dose rate and iso-effect relationships for normal tissue responses*, Int. J. Radiat. Oncol. Biol. Phys. **8**, 1981 (1982)
 - [13] A. van der Kogel, *Chronic effects of neutrons and charged particles on spinal cord, lung, and rectum*, Radiat. Res. Suppl. **8**, S208 (1985)
 - [14] J. Peck and F. Gibbs, *Mechanical assay of consequential and primary late radiation effects in murine small intestine: alpha/beta analysis*, Radiat. Res. **138**, 272 (1994)
 - [15] J. Taylor and D. Kim, *The poor statistical properties of the Fe-plot*, Int. J. Radiat. Biol. **56**, 161 (1989)
 - [16] R. de Boer, *The use of the D versus dD plot to estimate the alpha/beta ratio from iso-effect radiation damage data*, Radiother. Oncol. **11**, 361 (1988)
 - [17] L. Garcia, J. Leblanc, D. Wilkins, and G. Raaphorst, *Fitting the linear-quadratic model to detailed data sets for different dose ranges*, Phys. Med. Biol. **51**, 2813 (2006)
 - [18] D. Brenner, *et al.*, *The linear-quadratic model and most other common radiobiological models result in similar predictions of time-dose relationships*, Radiat. Res. **150**, 83 (1998)
 - [19] S. Curtis, *Lethal and potentially lethal lesions induced by radiation - a unified repair model*, Radiat. Res. **106**, 252 (1986)
 - [20] R. Hawkins, *A microdosimetric-kinetic model of cell death from exposure to ionizing radiation of any LET, with experimental and clinical applications*, Int. J. Radiat. Biol. **69**, 739 (1996)
 - [21] G. Obaturov, V. Moiseenko, A. Filimonov, *Model of mammalian cell reproductive death. I. Basic assumptions and general equations*, Radiat. Environ. Biophys. **32**, 285 (1993)
 - [22] C. Tobias, *The repair-misrepair model in radiobiology: comparison to other models*, Radiat. Res. Suppl. **8**, S77 (1985)
 - [23] R. Hawkins, *A microdosimetric-kinetic theory of the dependence of the RBE for cell death on LET*, Med. Phys. **25**, 1157 (1998)
 - [24] M. Zaider, *There is no mechanistic basis for the use of the linear-quadratic expression in cellular survival analysis*, Med. Phys. **25**, 791 (1998)
 - [25] R. Hawkins, *Effect of heterogeneous radiosensitivity on the survival, alpha beta ratio and biologic effective dose calculation of irradiated mammalian cell populations*, Clin. Transl. Radiat. Oncol. **4**, 32 (2017)
 - [26] Sachs RK and D. Brenner, *The mechanistic basis of the linear-quadratic formalism*, Med. Phys. **25**, 2071 (1998)
 - [27] D. Brenner, *The linear-quadratic model is an appropriate methodology for determining isoeffective doses at large doses per fraction*, Semin. Radiat. Oncol. **18**, 234 (2008)
 - [28] J. Kirkpatrick, D. Brenner and C. Orton, *The linear-quadratic model is inappropriate to model high dose per fraction effects in radiosurgery*, Med. Phys. **36**, 3381 (2009)

- [29] R. Hawkins, *A Microdosimetric-Kinetic model for the effect of non-Poisson distribution of lethal lesions on the variation of RBE with LET*, Radiat. Res. **160**, 61 (2003)
- [30] X. Harrison, *Using observation-level random effects to model overdispersion in count data in ecology and evolution*, PeerJ, **2**, e616 (2014)
- [31] G. Iliakis, T. Murmann and A. Soni, *Alternative end-joining repair pathways are the ultimate backup for abrogated classical non-homologous end-joining and homologous recombination repair: implications for the formation of chromosome translocations*, Mutat. Res. Toxicol. Environ Mutagen, **793**, 166 (2015)
- [32] S. Shelke and B. Das, *Dose response and adaptive response of non-homologous end joining repair genes and proteins in resting human peripheral blood mononuclear cells exposed to radiation*, Mutagenesis, **30**, 365 (2015)
- [33] R. Hawkins, *Biophysical Models, Microdosimetry and the Linear Quadratic Survival Relation*, Ann. Radiat. Ther. Oncol. **1**, 1013 (2017)
- [34] J. Ward, *DNA Damage Produced by Ionizing Radiation in Mammalian Cells: Identities, Mechanisms of Formation, and Reparability* Prog, Nucleic Acid Res. Mol. Biol. **35**, 95 (1988)
- [35] D. Goodhead, *Initial events in the cellular effects of ionizing radiations: Clustered damage in DNA*, Int. J. Radiat. Biol. **65**, 7 (1994).
- [36] J. Heilmann, G. Taucher-Scholz and G. Kraft, *Induction of DNA double-strand breaks in CHO-K1 cells by carbon ions*, Int. J. Radiat. Biol. **68**, 153 (1995)
- [37] E. Gudowska-Nowak, M. Kramer, G. Kraft and G. Taucher-Scholz, *Compound Poisson Statistics and Models of Clustering of Radiation Induced DNA Double Strand Breaks*. arXiv:physics/0011071v1 [physics.bio-ph] (2000)
- [38] R. Virsik and D. Harder, *Statistical interpretation of the overdispersed distribution of radiation-induced dicentric chromosome aberrations at high LET*, Radiat. Res. **85**, 13 (1981)
- [39] E. Goodwin, E. Blakely and C. Tobias, *Chromosomal damage and repair in G1-phase Chinese hamster ovary cells exposed to charged-particle beams*. Radiat. Res. **138**, 343 (1994)
- [40] T. Elsasser, et al., *Quantification of the relative biological effectiveness for ion beam radiotherapy: direct experimental comparison of proton and carbon ion beams and a novel approach for treatment planning*, Int. J. Radiat. Oncol. Biol. Phys. **78**, 1177 (2010)
- [41] T. Friedrich T, U. Scholz, T. Elsasser, M. Durante M and M. Scholz, *Calculation of the biological effects of ion beams based on the microscopic spatial damage distribution pattern*, Int. J. Radiat. Biol. **88**, 103 (2012)
- [42] R. Hawkins, *A statistical theory of cell killing by radiation of varying linear energy transfer*. Radiat. Res. **140**, 366 (1994)
- [43] T. Inaniwa, et al., *Treatment planning for a scanned carbon beam with a modified microdosimetric kinetic model*, Phys. Med. Biol. **55**, 6721 (2010)
- [44] D. Carlson, R. Stewart, V. Semenenko and G. Sandison, *Combined use of Monte Carlo DNA damage simulations and deterministic repair models to examine putative mechanisms of cell killing*, Radiat. Res. **169**, 447 (2008)
- [45] M. Frese, V. Yu, R. Stewart and D. Carlson, *A mechanism-based approach to predict the relative biological effectiveness of protons and carbon ions in radiation therapy*, Int. J. Radiat. Oncol. Biol. Phys. **83**, 442 (2012)
- [46] S. Streitmatter, R. Stewart, P. Jenkins and T. Jevremovic T, *DNA double strand break (DSB) induction and cell survival in iodine-enhanced computed tomography (CT)*, Phys. Med. Biol. **62**, 6164 (2017)
- [47] W. Wang, et al., *Modelling of cellular survival following radiation-induced DNA double-strand breaks*, Sci. Rep. **8**, 16202 (2018)
- [48] C. Karge and P. Peschke, *RBE and related modeling in carbon-ion therapy*, Phys. Med. Biol. **63**, 01TR02 (2017).
- [49] S. McMahon, J. Schuemann, H. Paganetti and K. Prise, *Mechanistic modelling of DNA repair and cellular survival following radiation-induced DNA damage*, Sci. Rep. **6**, 33290 (2016)
- [50] V. Semenenko and R. Stewart, *Fast Monte Carlo Simulation of DNA Damage Formed by Electrons and Light Ions* Phys, Med. Biol. **51**, 1693 (2006)
- [51] R. Stewart RD, et al., *Rapid MCNP simulation of DNA double strand break (DSB) relative biological effectiveness (RBE) for photons, neutrons, and light ions*, Phys. Med. Biol. **60**, 8249 (2015)
- [52] R. Stewart, *Induction of DNA damage by light ions relative to ^{60}Co gamma-rays*, Int. J. Part. Ther. **5**, 25 (2018)
- [53] T. Friedrich et al., *Systematic analysis of RBE and related quantities using a database of cell survival experiments with ion beam irradiation*, J. Radiat. Res. **54**, 494, (2013)
- [54] H. Paganetti et al., *Relative biological effectiveness (RBE) values for proton beam therapy*, Int. J Radiat. Oncol. Biol. Phys. **53**, 407 (2002)
- [55] H. Paganetti et al., *Relative biological effectiveness (RBE) values for proton beam therapy. Variation as a function of biological endpoints, dose, and linear energy transfer*, Phys. Med. Biol. **59**, R419 (2006)
- [56] G. Giovannini et al., *Variable RBE in proton therapy: Comparison of different model predictions and their influence on clinical-like scenarios*, Radiat. Oncol. **11**, 68 (2016)
- [57] C. van Leeuwen et al., *The alpha and beta of tumours: A review of parameters of the linear-quadratic model, derived from clinical radiotherapy studies*, Radiat. Oncol. **13**, 96 (2018)
- [58] M. Carante and F. Ballarini, *Modelling cell death for cancer hadrontherapy*, AIMS Biophysics, **4**, 465 (2017)
- [59] Y. Furusawa, et al., *Inactivation of aerobic and hypoxic cells from three different cell lines by accelerated ^3He -, ^{12}C - and ^{20}Ne -Ion beams*, Radiat. Res. **154**, 485 (2000)
- [60] R. Stewart, et al., *A comparison of mechanism-inspired models for particle relative biological effectiveness (RBE)*, Med. Phys. **45**, e928 (2018)
- [61] M. Butkus, R. Stewart, Z. Chen Z and D. Carlson, *Double strand break (DSB) complexity and proximity effects within the repair-misrepair fixation (RMF) model for improved predictions of cell survival from heavy ions*, Med. Phys. **45**, e532

- (2018)
- [62] D. Goodhead, *Initial events in the cellular effects of ionizing radiations: clustered damage in DNA*, Int J. Radiat. Biol. **65**, 7 (1994)
- [63] M. Hada, A. Georgakilas, *Formation of clustered DNA damage after high-LET irradiation: a review*, J. Radiat. Res. **49**, 203 (2008)
- [64] D. Goodhead, *Fifth Warren K. Sinclair keynote address: issues in quantifying the effects of low-level radiation*, Health Phys. **97**, 394 (2009)
- [65] A. Davis and D. Chen, *Complex DSBs: a need for resection*, Cell Cycle, **13**, 3796 (2014)
- [66] A. Hufnagel, *et al.*, *The link between cell cycle dependent radiosensitivity and repair pathways: a model based on the local, sister-chromatid conformation dependent switch between NHEJ and HR*, DNA Repair, **27**, 28 (2015)
- [67] M. Folkard, *et al.*, *Inactivation of V79 cells by low-energy protons, deuterons and helium-3 ions*, Int. J. Radiat. Biol. **69**, 796 (1996)

Appendix A

We use a customized negative binomial (NB) distribution for evaluating the probability of observing k lethal lesions in a cell

$$P_{NB}(k) = \frac{\Gamma(k+1/r)}{\Gamma(1/r) \times k!} \left(\frac{1}{1+r\mu} \right)^{1/r} \times \left(\frac{1}{1+1/r\mu} \right)^k. \quad (\text{A1})$$

The likelihood function for N iid observations (k_1, k_2, \dots, k_N) is given by

$$L_{NB} = \prod_{i=1}^N f(k_i)$$

from which the log-likelihood function can be written as:

$$\begin{aligned} l_{NB} = & -\left(\frac{1}{r}\right) \times (1+k+r) \times \ln(1+r+\mu) + \\ & k \times \left(\ln(r) + \ln(\mu) \right) + \ln \left[\Gamma\left(\frac{1+k+r}{r}\right) \right] - \\ & \ln[\Gamma(1+k)] - \ln \left[\Gamma\left(\frac{1}{r}\right) \right]. \end{aligned} \quad (\text{A2})$$

Assuming that the correct repair distribution is NB distributed, the probability that a break will be repaired correctly is

$$\begin{aligned} P_{NB} &= \sum_{k=0}^{\infty} \frac{1}{1+k} P_{NB}(k) \\ &= \sum_{k=0}^{\infty} \frac{\Gamma(k+\omega)}{\Gamma(\omega)} \times \frac{1}{1+k} p^{\omega} (1-p)^k \\ &= \sum_{k=0}^{\infty} \frac{(k+\omega-1)!}{(\omega-1)!(k+1)!} p^{\omega} (1-p)^k \end{aligned} \quad (\text{A3})$$

If we let $k+1=s$ and $\omega-1=z$, then

$$\begin{aligned} P_{correct} &= \frac{p}{z(1-p)} \sum_{s=1}^{\infty} \frac{(s+z-1)!}{s!(z-1)!} p^z (1-p)^s \\ &= \frac{p}{(\omega-1)(1-p)} (1-p^{\omega-1}) \end{aligned} \quad (\text{A4})$$

By fixing the average number of breaks equal to the expected interaction rate $\mu = \eta(\lambda_p)n_p$, we can use this to calculate the total probability of misrepair as a function of λ_p . Using $p = 1/(1+\omega\mu)$, we expand Eq. (A4) to obtained

$$P_{NB} = \omega \left(1 - \frac{1}{2} \eta(\lambda_p)n_p \right). \quad (\text{A5})$$